Computationally Efficient Winding Loss Calculation with Multiple Windings, Arbitrary Waveforms, and Two-Dimensional or Three-Dimensional Field Geometry

Charles R. Sullivan, *Member, IEEE*

***Abstract*—The squared-field-derivative method for calculating eddy-current (proximity-effect) losses in round-wire or litz-wire transformer and inductor windings is derived. The method is capable of analyzing losses due to two-dimensional and three-dimensional field effects in multiple windings with arbitrary waveforms in each winding. It uses a simple set of numerical magnetostatic field calculations, which require orders of magnitude less computation time than numerical eddy-current solutions, to derive a frequency-independent matrix describing the transformer or inductor. This is combined with a second, independently calculated matrix, based on derivatives of winding currents, to compute total ac loss. Experiments confirm the accuracy of the method.**

***Index Terms*—Eddy currents, finite-element methods, inductors, magnetic devices, numerical field computation, power conversion, power transformers, proximity effect, skin effect.**

I. Introduction

EDDY-CURRENT losses, including skin-effect and proximity-effect losses, seriously impair performance of transformers and inductors in high-frequency power conversion applications. Avoiding or mitigating these high-frequency winding losses is one of the most important considerations in designing such components. Unfortunately, standard methods of analyzing winding loss have significant limitations. In particular, standard analytical methods [1]–[18] ([16] gives a useful review) assume a one-dimensional (1-D) field for analyzing eddy-current effects in windings. But two-dimensional (2-D) effects are important in magnetic components that include discrete air gaps, in short windings where end effects are significant, or in non layer-based windings. Finite-element or other numerical field-calculation methods can account for 2-D effects, but their direct use to calculate eddy-current effects in windings is computationally expensive. In this paper, we introduce a method that includes the effects of 2-D or three-dimensional (3-D) fields with a much lower computational cost. The new method, which we term the *squared-field-derivative* (SFD) method, can easily take into account multiple windings and nonsinusoidal waveforms that may be different in each winding. For frequencies in a range where the method is valid, it produces a frequency-independent model that may be used to calculate losses for any set of waveforms. The method applies to round-wire windings, including litz-wire windings, but is not intended to address foil windings. For multi-filar or "n-in-hand" windings, in which the interleaving of different windings occurs at the level of individual turns, the method could be applied, but its advantages are less significant than they are for windings in which more turns of a particular winding are grouped together.

Manuscript received January 18, 2000; revised September 15, 2000. This work was supported in part by West Coast Magnetics. Recommended by Associate Editor K. Ngo.

The author is with Thayer School of Engineering, Dartmouth College, Hanover, NH 03755 USA (e-mail: charles.r.sullivan@dartmouth.edu).

Publisher Item Identifier S 0885-8993(01)00974-7.

A. Review of Previous Analytical Approaches

Although different descriptions can be used, most existing analytical calculations of high-frequency wire-winding loss are fundamentally equivalent to one of three analyses. The most rigorous approach uses an exact calculation of losses in a cylindrical conductor with a known current, subjected to a uniform external field, combined with an expression for the field as a function of 1-D position in the winding area [6], [18]. Perhaps the most commonly cited analysis [7] uses "equivalent" rectangular conductors to approximate round wires, and then proceeds with an exact 1-D solution. Finally, there is the option of using only the first terms of a series expansion of these solutions, e.g., [15], [19], [20].

For designs in which 1-D field analysis is accurate, and where wire strands are not large compared to a skin-depth, these various methods are approximately equivalent [6], despite one small discrepancy explained in [21]. Although the basic analysis is usually based on sinusoidal waveforms, a number of authors have developed methods of extending this analysis to nonsinusoidal waveforms through Fourier analysis or other methods [11], [13], [19], [20]–[23].

A major limitation of all of this work is that it only applies to components in which the field geometry is 1-D. This excludes nearly all inductors and gapped transformers, in which the 2-D field geometry due to the gap significantly affects losses [24]. Standard 1-D analysis is also unable to analyze transformers with 2-D winding layout, such as the one shown in Fig. 1. In [25] an analytical approach is developed for 2-D fields in gapped single-winding inductors. Unlike the SFD method, it applies to only one particular geometry. Nonetheless, the geometry analyzed is widely used, and it is a valuable method that can be considered complimentary to the SFD method, in that it applies

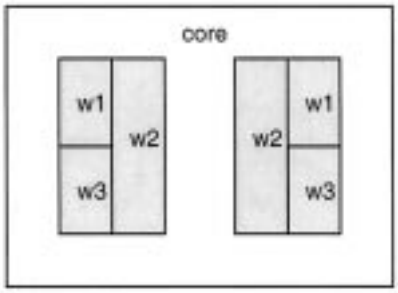

Fig. 1. Example of an ungapped three-winding transformer (w1–w3) in which 2-D field geometry can be important.

primarily to foil windings, whereas the SFD method is for wire windings.

B. Limitations of General-Purpose Electromagnetic Analysis

Work in computational electromagnetics has produced general-purpose field analysis methods, and commercial software is available for 2-D and 3-D solutions of arbitrary problems, including analysis of eddy currents. However, there are two major limitations of this approach for high-frequency magnetics in power electronics applications.

Scale Problems: Transformers and inductors often require many turns of fine wire, or may use stranded wire such as litz wire to reduce eddy-current losses. The wire strands may be as small as 30–50 μm in diameter (44–48 AWG), while the overall dimensions may be tens of centimeters. Thus, the length scales involved can vary over two to four orders of magnitude, and there are often thousands, or even over a hundred thousand strands of wire in a winding window (e.g., see [26]). Even when larger wire is used, the skin depth in the wire can be small, for example 100 μm at 400 kHz, creating a similar disparity of length scales. In either case a large number of elements are needed to perform finite-element analysis, and this leads to slow simulations and large memory requirements. To circumvent this problem, software vendors recommend modeling a stranded winding as a region of uniform current density. While this is helpful for analyzing field distributions, it provides no information on losses in the stranded winding.

Optimization: With existing field analysis, optimization must be done by trial and error. Particularly when each iteration takes hours to analyze via finite-element analysis, true optimization is not practical, except in a few academic experiments, which typically then provide information only about one particular design. In some work [27], [28], systematic numerical simulations have been used to develop models with more general application. The results in [27], [28] apply to foil windings, and thus are complimentary to the SFD method, which applies only to wire windings.

II. The Squared-Field-Derivative Method

In order to circumvent both the limitations of 1-D analytical methods, and the limitations of existing numerical methods, we use a combination of numerical calculation of the overall field geometry with analytical calculation of its interaction with the winding strands. This avoids the scale problem, but allows applying the power of modern computers to quickly obtain a much more accurate solution than would be available through 1-D analysis. A similar approach was described in [17] and was also used in [29] for gapped single-winding inductors with sinusoidal waveforms.

We start with the calculation of loss in a conducting cylinder in a uniform field, perpendicular to the axis of the cylinder, with the assumption that the field remains constant inside the conductor, equivalent to the assumption that the diameter is not large compared to a skin depth. This restriction might seem to limit applicability to situations in which ac loss is negligible. However, it is well known that ac losses can become severe even with this restriction, particularly for multi-layer windings (see, for example, [15]). As shown in Appendix A, a calculation of eddy current based on a uniform field within the cylinder results in instantaneous power dissipation $P(t)$ in a wire of length ℓ

$$P(t) = \frac{\pi \ell d_c^4}{64 \rho_c} \left(\frac{dB}{dt} \right)^2 \tag{1}$$

where

B flux density, assumed perpendicular to the axis of the cylinder;
ρ_c resistivity of the wire;
d_c diameter.

The average loss depends on the time average of the squared derivative of the field, $\overline{(dB/dt)^2}$ (Hence the term *squared-field-derivative*, or SFD). The squared field derivative, or corresponding squared winding current derivatives, have been used by many authors, including [19]–[21], [23]. The "K-factor" used in rating low-frequency power transformers for nonsinusoidal currents can also be understood on the same basis [30]. In this paper, the squared field derivative is used to develop a method that extends the domain to which this approach can be applied.

To calculate the time average of total ac loss in all the conductors of a winding, we can use the spatial average of the time-averaged squared field derivative

$$P_{e,j} = \frac{\pi \ell_{t,j} N_j d_{c,j}^4}{64 \rho_c} \left\langle \overline{\left(\frac{dB}{dt} \right)^2} \right\rangle_j \tag{2}$$

where

$P_{e,j}$ time average ac (eddy-current) loss in winding j;
N_j number of turns in winding j;
$\ell_{t,j}$ average length of a turn;
$\langle \cdot \rangle_j$ spatial average over the region of winding j;
$\overline{\cdot}$ time average.

For a litz-wire winding, N_j should represent the product of the number of turns and the number of strands in each turn (i.e., N_j is the total number of strands in the winding), and d_c is the diameter of the individual strands. The length of a turn may also need to be adjusted to account for the increased distance that a strand travels on account of twisting. This calculation of ac loss in litz wire neglects eddy currents circulating between strands (bundle-level effects), and considers only eddy currents circulating within individual strands (strand-level effects), which is usually valid because with proper bundle construction, bundle-level effects can be made negligible [21].

In a given winding, the field, $\vec{B}$ may be expressed as the superposition of fields due to currents in each winding. We can then express the loss in winding j of a two-winding transformer as

$$P_{e,j} = \gamma_j \left\langle \overline{\left|\frac{d\vec{B}_1}{dt}\right|^2} + \overline{\left(\frac{d\vec{B}_1}{dt}\right)\cdot\left(\frac{d\vec{B}_2}{dt}\right)} + \overline{\left(\frac{d\vec{B}_2}{dt}\right)\cdot\left(\frac{d\vec{B}_1}{dt}\right)} + \overline{\left|\frac{d\vec{B}_2}{dt}\right|^2} \right\rangle_j \tag{3}$$

where γ_j is a loss constant defined as

$$\gamma_j = \frac{\pi N_j \ell_{t,j} d_{c,j}^4}{64\rho_c} \tag{4}$$

and $\vec{B}_k$ is the field due to current in winding k. In a typical situation of interest, the field due to the current in a given winding may be considered to be instantaneously proportional to that current, equal to the field that would be obtained with a dc current the same as the instantaneous value of the time-varying current. As will be discussed in more detail in Section IV, this approximation is valid given the assumption, introduced above, that the wire diameter is not large compared to a skin depth. With the fields proportional to the currents, it is possible to express the loss in terms of the currents as

$$P_{e,j} = a_{j,11}\overline{\left(\left(\frac{di_1}{dt}\right)^2\right)} + a_{j,12}\overline{\left(\frac{di_1}{dt}\frac{di_2}{dt}\right)} + a_{j,21}\overline{\left(\frac{di_2}{dt}\frac{di_1}{dt}\right)} + a_{j,22}\overline{\left(\left(\frac{di_2}{dt}\right)^2\right)} \tag{5}$$

where $a_{j,mn}$ is a constant relating current and loss, to be calculated in the next section. Note that the loss in one winding results from the total field in that winding, which may be affected by currents in any winding. Thus, the expression for ac loss in a given winding (5) involves all winding currents. The total ac loss in all windings is the sum of such terms for each winding, and can be expressed as

$$P_{e,total} = \overline{\begin{bmatrix} \frac{di_1}{dt} & \frac{di_2}{dt} \end{bmatrix} \mathbf{D} \begin{bmatrix} \frac{di_1}{dt} \\ \frac{di_2}{dt} \end{bmatrix}} \tag{6}$$

where $\mathbf{D}$ is the sum of the matrices a_{mn} for each winding

$$\mathbf{D} = \sum_j a_{j,mn}. \tag{7}$$

$\mathbf{D}$ can be termed a dynamic resistance matrix, and carries units of Ω-s^2. The meaning of the different elements of $\mathbf{D}$ can be understood with reference to the idea of self and mutual ac resistance [31]. The diagonal elements of $\mathbf{D}$ reflect the eddy-current-loss contribution to the self resistance of the windings, and the off-diagonal elements reflect the mutual resistance.

An advantage of this formulation is that the matrix $\mathbf{D}$ may be calculated from a set of magnetostatic field calculations for the transformer geometry (see the following section), without specifying the waveforms or frequency of operation. The matrix

$$\overline{\begin{bmatrix} \frac{di_1}{dt} \\ \frac{di_2}{dt} \end{bmatrix} \begin{bmatrix} \frac{di_1}{dt} & \frac{di_2}{dt} \end{bmatrix}} \tag{8}$$

may be independently calculated for the particular set of waveforms of interest. Then the inner product of these two matrices yields the total ac loss. To calculate total transformer loss, one must combine this figure with core loss and winding loss due to dc winding resistance ($R_{\rm dc} I_{\rm rms}^2$). This formulation illustrates the contribution of the high slopes often used in power electronics to winding loss, and the importance of measuring or predicting these slopes, and then representing them accurately.

This analysis may be extended in the obvious way to an arbitrary number of windings, and is shown above for two windings only to simplify the presentation.

III. Field Calculations

The matrix $\mathbf{D}$ needed for the above loss calculation can be shown to be

$$\mathbf{D} = \gamma_1 \left\langle \begin{bmatrix} \left|\hat{\vec{B}}_1\right|^2 & \hat{\vec{B}}_1 \cdot \hat{\vec{B}}_2 \\ \hat{\vec{B}}_2 \cdot \hat{\vec{B}}_1 & \left|\hat{\vec{B}}_2\right|^2 \end{bmatrix} \right\rangle_1 + \gamma_2 \left\langle \begin{bmatrix} \left|\hat{\vec{B}}_1\right|^2 & \hat{\vec{B}}_1 \cdot \hat{\vec{B}}_2 \\ \hat{\vec{B}}_2 \cdot \hat{\vec{B}}_1 & \left|\hat{\vec{B}}_2\right|^2 \end{bmatrix} \right\rangle_2 \tag{9}$$

where $\hat{\vec{B}}_j$ is the field everywhere due to a unit current in winding j, and $\langle \cdot \rangle_j$ is the spatial average over the region of winding j. In order to find this we may calculate the fields due to current in each winding individually. Then the quantities $< \vec{B}_j \cdot \vec{B}_k >_m$ and $< |\vec{B}|_j^2 >_k$ may be calculated from these fields.

The field calculations, which are the same calculations needed to determine an inductance matrix for the transformer, may be done using any magnetostatic finite-element analysis program, or by specialized methods that are more efficient for a particular problem, such as those discussed in [17] and [29]. Depending on the geometry involved and the accuracy required, the calculation may be 2-D (in Cartesian or cylindrical coordinates) or 3-D. In the 3-D case, the field may not always be perpendicular to the axis of the wire, resulting in slightly lower loss in practice than the calculations presented here would predict. Although a correction for this could be made, few practical geometries have significant field components parallel to the path of the wire. In most cases, the field calculation can be simplified because it is not necessary to model the individual turns of the windings. It suffices to model the overall region of the winding as a region of constant current density. The computational requirements are thus greatly reduced compared to a full eddy-current simulation: The geometry modeled is simpler, the simulation need not include eddy currents, and the simulation does not need to be repeated for different frequencies.

TABLE I
CONSIDERATIONS LIMITING SCOPE OF APPLICATION

Consideration	Requirement	Practical Rule of Thumb For When the SFD Method Applies — indicates that the requirement is satisfied in most practical situations
Validity of (1) (loss model)	Round wires, d_c not $>> \delta$	Round wire including litz wire. Up to frequencies where $d_c = 2\delta$.
Validity of magnetostatic simulation	2D simulation an adequate approximation, if used.	Be aware of 3D effects and use 3D simulation if necessary.
	3D field component parallel to wire should be small.	—
	Equal current sharing between litz strands.	Any litz wire must use proper construction to avoid bundle-level skin effect.
	Known current sharing between parallel windings.	Treat parallel windings separately unless symmetry guarantees current sharing.
	Capacitive currents small relative to other currents.	Frequencies below one-third the resonant frequency in an inductor.
	Hysteresis doesn't affect winding field.	—

Irrespective of the field calculation method, the approach we have described for finding the value of $\mathbf{D}$ entails calculating and storing the complete field information $\hat{\vec{B}}_1(\vec{x})$ and $\hat{\vec{B}}_2(\vec{x})$, and then finding the winding-region spatial averages of the square terms and of the cross products. An alternative that requires less data storage and may be more convenient with the user interfaces of some commercial finite-element packages is to calculate the field with current in each winding individually, perform the necessary averages, and then calculate the field with current in both windings, repeat the averaging, and subtract to find the cross terms.

IV. ASSUMPTIONS AND SCOPE OF APPLICATION

The SFD method allows analysis of a wider range of winding types than do previous methods; it allows both arbitrary waveforms and 2-D or 3-D field geometries. However, there are a number of assumptions that have been made in the analysis. Most of these were noted in the derivation; we repeat them here for clarification of how they limit the scope of the SFD method, and to discuss prospects for extending the scope. The considerations discussed here are summarized in Table I.

The analysis is based on round wires. Other shapes could be analyzed by similar methods, as long as all the dimensions were small compared to the winding window. However, the loss would then depend on the orientation of the field, somewhat complicating calculations. In the case of litz wire, we have assumed that bundle-level effects are negligible, a valid assumption for well-designed litz constructions [21]. We have also assumed that the wire (or strand, in the case of litz wire) is small compared to a skin depth. If it is not, a similar approach could be used, combining magnetostatic field calculations with Bessel-function analysis of the loss in the winding [6], [17], [18]. Unfortunately, this results in a frequency-dependent matrix $\mathbf{D}$, so it is preferable to use (1) when possible. It is also important to note that if the wire is large compared to a skin depth, the eddy currents are significantly affecting the field within the wire, and may also significantly affect the overall field distribution. Thus, it may also be necessary to modify the magnetostatic analysis to account for the effect the eddy currents have on the field distribution, unless the winding packing factor is very small, or the winding window region of the core is completely filled by windings of uniform strand size and packing factor.

The use of 2-D field calculations entails a degree of approximation that depends on the importance of 3-D effects in the particular geometry under study. If necessary, 3-D calculations may be used. This still entails a minor approximation: The loss induced by a field parallel to the axis of the wire is less than the loss we calculate assuming a perpendicular field. In most geometries of interest, the parallel component of the field is small. If it were significant, the loss prediction would be slightly high, leading to a conservative design.

In order for the magnetostatic field analysis to be valid, the current distribution between different conductors must be constant, independent of frequency. In the case of litz wire, construction can guarantee current sharing between strands independent of frequency [21]. Paralleled windings in different physical positions may not share ac current equally, so unless symmetry guarantees equal sharing, they should be modeled as separate windings for accurate evaluation with the SFD method. In a single winding, capacitive currents between layers may become significant at high frequencies, such that the current is different in each turn. This can alter the field, and a new field calculation based on the current distribution with capacitive effects included would be needed to evaluate loss with the SFD method. However, this is rarely needed, as high capacitive currents would cause other circuit problems such as EMI and switching losses, and so designs are limited to lower capacitance by other considerations.

Finally, we also note that the use of a magnetostatic field calculation is based on the assumption that hysteresis in the core does not significantly affect the field in the window area. Such an effect would only happen with extremely high hysteresis loss, and so is not likely to be a problem in any power applications. (The hysteresis loss would need to be significant compared to the VA handled by the inductor or transformer, not just compared to other losses.)

In summary, most of the assumptions discussed above are nearly always valid for round wire windings and properly-constructed litz wire, up to a maximum frequency which is the lower of two limits: where the skin depth becomes small compared to the conductor size, or where capacitive currents become a significant fraction of the winding current. In an inductor, or a

TABLE II
TRANSFORMER USED FOR VERIFICATION

Windings		
	Number of turns	33:33
	Number of layers in each winding	1.5
	Wire type	3x8/36 litz
	Number of strands in each turn	24
	Strand gauge	36 AWG
Core		
Geometry	Round-center-post EE	ETD39
Material	MnZn Ferrite	TDK PC40
Gap	Centerpost and outer legs	3 mm (6 mm total)

transformer with a two-terminal excitation, the latter frequency limit is equivalent to requiring operation well below the resonant frequency (e.g., at or below one-third the resonant frequency, where capacitive current is an order of magnitude below the inductive current). It is also important to note that parallel windings must be treated separately unless symmetry guarantees current sharing between them.

V. VERIFICATION

Initial experiments for verification of the squared-field-derivative method, reported in [32], used a two-winding litz-wire transformer. Simulations and experiments were performed with and without a gapped core. Although the air-core results very closely matched the predictions made by the SFD method, the results with the gapped core began to deviate at frequencies as low as 60 kHz. The deviation was attributed to winding capacitance which both complicates the extraction of winding resistance (see Section V-B), and changes the current distribution in the winding window as discussed in Section IV. In order to confirm this explanation for the discrepancies, a transformer with a similar geometry and similar potential for eddy-current losses, but with a much higher resonant frequency, was simulated, constructed and tested. As detailed below, predicted and experimental results match very closely for this transformer, confirming the validity of the SFD method, and confirming the diagnosis of the problems observed in [32].

Parameters of the new transformer are listed in Table II. It would be very difficult to predict winding losses in this transformer without the SFD method, because, as in the original transformer tested in [32], there are significant 2-D effects produced by the gap and the winding design (shown in Fig. 2), and because the large number of strands in the winding window (over 1500 total) would make direct simulation prohibitive. Large gaps (3 mm gaps in the centerpost and outer core legs) were used to minimize core loss relative to winding loss. Although long gaps might intuitively seem to magnify the effect of gap fringing fields on ac resistance, longer gaps actually slightly decrease the effect [27], [29]. Thus, in the configuration we measured, the effect of gap fringing field on loss is slightly milder than in a typical practical design, but is still quite significant, as shown below.

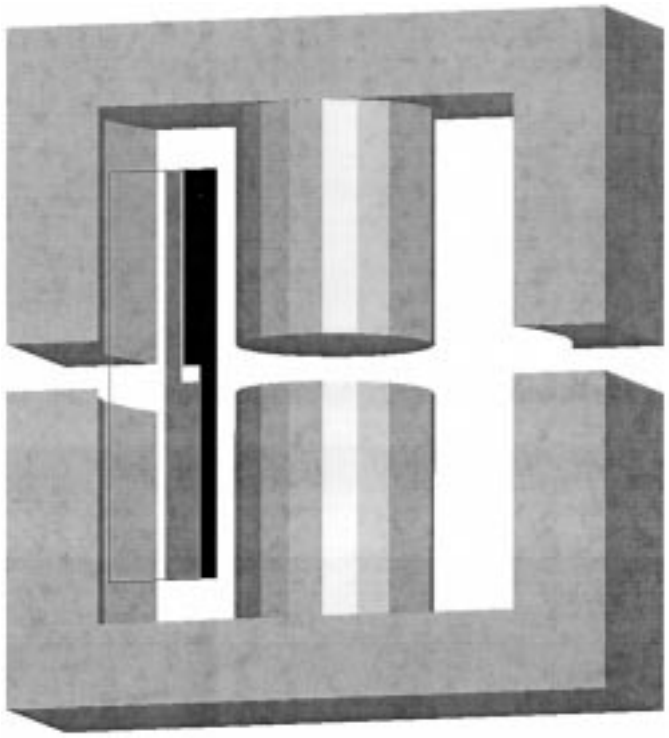

Fig. 2. Configuration of experimental transformer, showing the core, a cross section of each winding in the left window, and an outline of the bobbin area. The magnetostatic simulation used a constant current density in the winding regions shown (rotated around the centerpost to make a solid volume). Neither the 33 individual turns in each winding nor the 24 strands within each turn need to be represented explicitly. The figure is approximately twice actual size.

A. Field Calculations

Three 3-D magnetostatic simulations with a commercial finite-element package [33] were used to find the field values with current in each winding individually, and with current in both simultaneously. Each winding was modeling by a region of constant current density, as shown in Fig. 2. The individual turns within this region were not represented in the simulation. Automatic mesh refinement was used with a target error of under 1%. The software's postprocessor was used to find the average values of B^2 in each winding region, so that $\mathbf{D}$ could be calculated as described in Section III. The average turn length was calculated geometrically, and then adjusted upward by 5% to account for the strand length increase due to twisting in the litz bundle, based on measurements of the dc resistance of a length of the litz wire used. The resulting dynamic resistance matrix is

$$\mathbf{D} = \begin{bmatrix} 123 & 88.7 \\ 88.7 & 160 \end{bmatrix} \mathrm{m}\Omega(\mu\mathrm{s})^2. \tag{10}$$

The significant off-diagonal elements in this matrix illustrate the importance of the relationships between the different winding currents in determining ac winding loss. Even for sinusoidal waveforms, the common practice of calculating ac loss in a given winding as $I_{\mathrm{rms,\,ac}}^2 \cdot R_{\mathrm{ac}}$ is not adequate for a transformer; mutual resistance effects must be included [31].

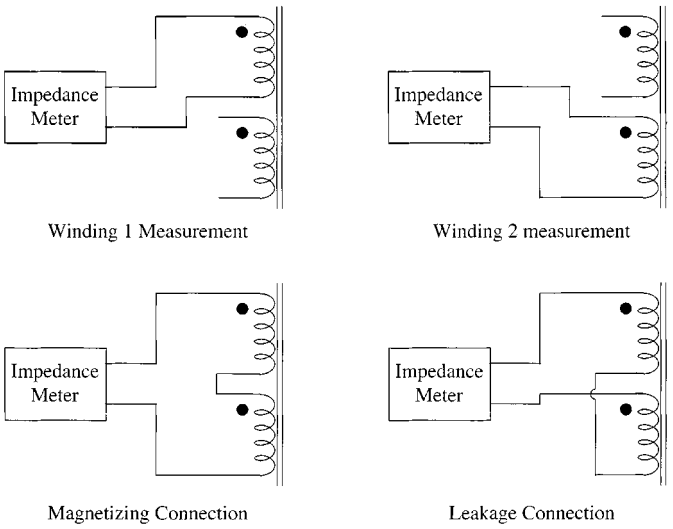

Fig. 3. Four winding connections measured.

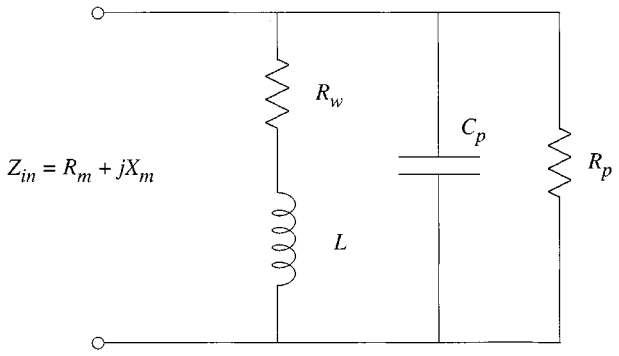

Fig. 4. Circuit representing winding impedance, used to interpret experimental measurements.

B. Measurements and Winding Resistance Extraction

With the matrix $\mathbf{D}$, the loss could be predicted for any waveforms. However, accurate measurements could be most easily obtained for sinusoidal waveforms, using an HP 4284A impedance analyzer. Verifying the effect of each term in the matrix $\mathbf{D}$ was possible by using different combinations of current in different windings, as shown in Fig. 3. The four combinations are as follows: each winding driven individually, and both driven in series with the same or opposite polarities (exciting the magnetizing or leakage inductance, respectively).

In order to determine the winding resistance from the measured impedance, the model shown in Fig. 4 was used. Here, C_p represents winding capacitance and R_p represents dielectric loss in this capacitance and core loss. The real part of the impedance of this network, R_m is what is measured. However, R_w is what is predicted by the analysis. To extract R_w from the measured data, we found values for C_p and R_p and used the relationship

$$R_m = \mathrm{Re}\left\{(R_w + j\omega L) \| \left(R_p \| \frac{1}{j\omega C_p}\right)\right\} \qquad (11)$$

where $\mathrm{Re}\{\cdot\}$ indicates the real part, to solve for R_w. Values for C_p were calculated from the self-resonant frequency of each winding or winding combination (Table III). Values for R_p were obtained by measuring impedance with a closed core and with the actual winding driven with the same voltage as in the winding resistance test. The value of R_p obtained from this measurement represents both core loss and dielectric or other loss in the winding capacitance.

TABLE III
WINDING RESONANT FREQUENCIES

Winding	f_0 with gapped ferrite core
Winding 1 (inner)	3.78 MHz
Winding 2 (outer)	3.82 MHz
Both–magnetizing connection	1.91 MHz
Both—leakage connection	6.45 MHz

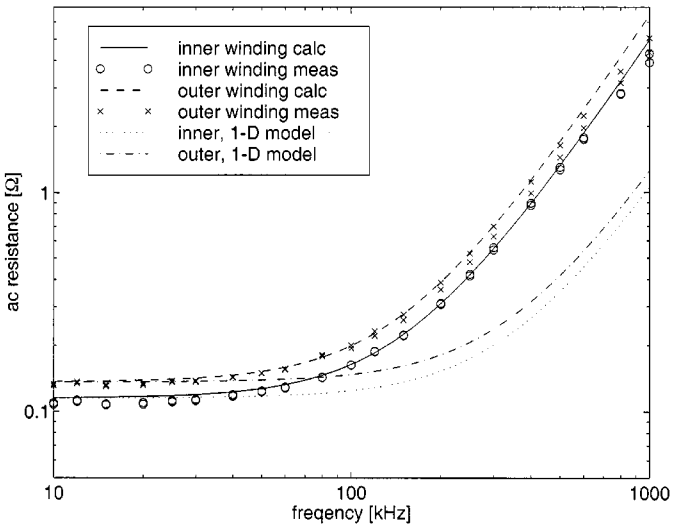

Fig. 5. Measured ac resistance of individual windings for the tested gapped-ferrite-core transformer, as corrected using (11), compared to the ac resistance predicted by the SFD method. Also shown as dotted lines are the ac resistances for the individual windings predicted by 1-D analysis, as described in Appendix II.

C. Results

The experimental results are compared with the SFD prediction in Figs. 5 and 6, for the frequency range of 10 kHz to 1 MHz. The results correspond very well over most of the frequency range. Two sets of data are shown, corresponding to two trials of the measurement, with independent calibration of the meter on each trial. (Calibration nulls the impedance of the leads used to connect the transformer.) At 1 MHz, several effects are expected to degrade the accuracy of the SFD method. The diameter of AWG 36 strands is larger than the skin depth, and, for the series magnetizing winding connection, a test frequency of 1 MHz is above one third the 2 MHz resonant frequency of the winding. At 1 MHz, the magnetizing connection does in fact show more significant deviation than the other connections do, consistent with the fact that 1 MHz is not as close to the other connections' resonant frequencies.

Figs. 5 and 6 also include loss predictions from simple 1-D analysis [15], [21], as detailed in Appendix II. In the plot of individual winding loss (Fig. 5), we see that the ac resistance with the gap fringing field is a factor of four higher than predicted

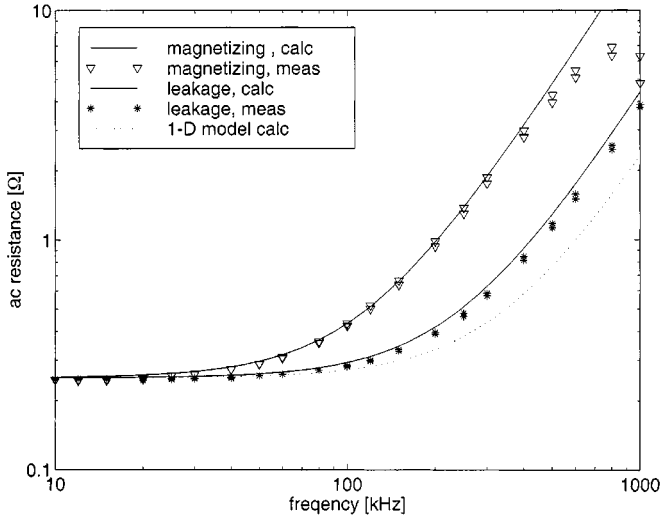

Fig. 6. Measured ac resistance of two series winding configurations for the tested gapped-ferrite-core transformer, as corrected using (11), compared to the ac resistance predicted by the SFD method. Also shown as a dotted line is the ac resistance factor predicted by 1-D analysis, which is the same for either polarity of series winding connection, as described in Appendix II.

by the 1-D analysis, and that this is correctly predicted by the SFD method. In Fig. 6 we see that the 1-D calculation is closer to correct for the leakage connection, because gap fringing is not significant for this excitation. However, it still has error of about 50% because of the 2-D winding configuration with each winding using one-and-a-half layers (Fig. 2). For the magnetizing connection, the 1-D analysis predicts the same resistance as for the leakage connection (for a transformer with gaps in the outer legs as well as the centerpost). But in practice, as correctly predicted by the SFD method, the ac resistance for the magnetizing connection is about a factor of six higher than the 1-D prediction.

The results illustrate that the SFD method is accurate in the frequency range where it is applicable (below one-third the winding resonant frequency and below the frequency where the skin depth becomes small compared to the conductor size). The SFD method has been experimentally demonstrated to have greatly improved accuracy in comparison to 1-D methods when gap fringing fields are significant, or when the winding geometry has significant 2-D aspects.

D. Computational Costs

The predictions were obtained with modest computational costs—the set of three 3-D simulations used took a total of 43 min with adaptive mesh refinement to a 1% error criterion. A comparison with a direct simulation was not possible, as the computational cost to perform a 3-D simulation with 1500 wire strands would have been prohibitive. However, a comparison was performed with a simpler design. The 2-D magnetostatic simulation required for the SFD method was compared to a full 2-D simulation of strand eddy currents in a 250 kHz inductor with 110 turns of 0.4 mm diameter wire. The magnetostatic analysis required for the SFD method took 6 s, whereas the full eddy-current analysis took over 18 min. Using a device with only 110 strands, as opposed to the 1500 strands in our experimental device, made this experiment possible, but also minimized the difference in simulation time.[1] The difference would be even more dramatic for more complex structures, for more strands, or for 3-D simulations. The test was based on the assumption of a sinusoidal current waveform. Non-sinusoidal waveforms would require no additional magnetostatic simulation time for the SFD method, but, for the full finite-element analysis of eddy currents, would require an additional, similar simulation for each harmonic.

VI. Conclusion

The SFD method allows calculating losses in multi-winding transformers with 2-D and 3-D field effects and arbitrary waveforms in each winding. It uses a simple set of magnetostatic field calculations to derive a matrix describing the transformer, independent of the excitation applied to the transformer. This is combined with a second matrix calculated from derivatives of winding currents to calculate total ac loss. Experiments show the method is highly accurate within the limits described in Section IV.

The dramatic decrease in computational expense made possible by using only simplified magnetostatic field calculations makes it possible to accurately predict loss in transformers or inductors that were previously beyond the capabilities of practical analysis. The increase in speed not only can make it easier to predict loss for a given design, but also can make numerical optimization practical. In addition, the way many parameters affect loss is made explicit. These explicit relationships are expected to be useful in analytical optimizations of winding and component design.

Appendix I
Loss in a Conduction Cylinder

This derivation of (1), the loss in a conducting cylinder with a changing flux perpendicular to the axis of the cylinder, is similar to that in [1], except that [1] expresses it in the frequency domain rather than the time domain. It is based on the geometry shown in Fig. 7. Consider an eddy-current loop down a section of the cylinder at position x and of thickness dx, returning in the corresponding section on the other side of the cylinder at $-x$, as shown. Assuming uniform flux density, B, perpendicular to the cylinder axis, the derivative of flux in this section, which is equal to the EMF induced around the loop, is

$$\frac{d\Phi}{dt} = 2x\ell\frac{dB}{dt} \tag{12}$$

where ℓ is the length of the cylinder (into the page in Fig. 7). The resistance of this path is

$$R = \frac{2\ell\rho_c}{2\sqrt{\frac{d^2}{4} - x^2}\,dx}. \tag{13}$$

[1]Both simulations used the same 2-D finite-element simulation package (Ansoft Maxwell) with adaptive mesh refinement and a 1% energy error criterion, running on a 300 MHz Pentium machine. The magnetostatic simulation was completed in 6 s, using less than 1 s of CPU time, whereas the full simulation took over 18 m of CPU time. Memory requirements were 1 MB and 16 MB, respectively.

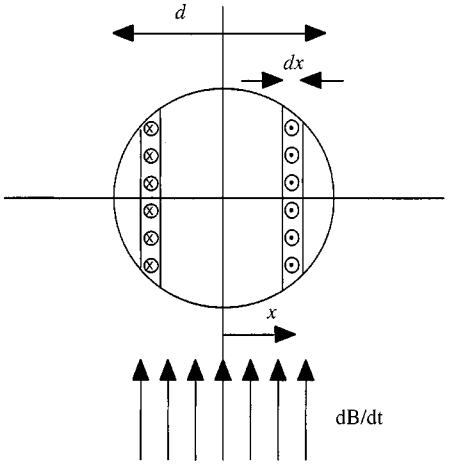

Fig. 7. Calculation of loss in a conducting cylinder with uniform flux density.

The power dissipated in these differential elements $((d\Phi/dt)^2/R)$ may be integrated to find the instantaneous total power loss in the cylinder, $P(t)$

$$P(t) = \int_0^{d/2} \left(2x\ell \frac{dB}{dt}\right)^2 \frac{\sqrt{\frac{d^2}{4} - x^2}}{\ell \rho_c}\, dx \tag{14}$$

$$= \frac{\pi \ell d_c^4}{64 \rho_c} \left(\frac{dB}{dt}\right)^2. \tag{15}$$

Appendix II
One-Dimensional Analysis Used for Comparison

For the purpose of a comparison in Figs. 5 and 6, a 1-D model was used. While no application of a 1-D model to this 2-D configuration is defensible, the following represents an attempt to apply one dimensional modeling as rigorously as possible. AC resistance factor $F_r = R_{\rm ac}/R_{\rm dc}$ is modeled by [15], [21]

$$F_r = 1 + \frac{\pi^2 \omega^2 \mu_0^2 N^2 n^2 d_c^6 k}{768 \rho_c^2 b_c^2} \tag{16}$$

where

- ω radian frequency of a sinusoidal current;
- n number of strands;
- N number of turns;
- d_c diameter of the copper in each strand;
- ρ_c resistivity of the copper conductor;
- b_c breadth of the window area of the core;
- k factor accounting for field distribution in multiwinding transformers, equal to one for windings that have zero MMF on one side [15].

For the experimental transformer discussed in Section V, with excitation of a single winding, half the MMF is dropped across the centerpost gap, and half the MMF is dropped across the outer gaps. Each half of the winding then has zero MMF on one side, and for the half-winding, $k = 1$, and N is half the total number of turns. Thus for each half-winding

$$F_r = 1 + \frac{\pi^2 \omega^2 \mu_0^2 (N/2)^2 n^2 d_c^6}{768 \rho_c^2 b_c^2} \tag{17}$$

and with equal values of F_r in each half-winding, the whole winding also has the same value of F_r. The result is shown in Fig. 5, where it can be seen that this one dimensional model does not accurately predict ac resistance for the transformer tested, because of its significant 2-D effects.

With magnetizing excitation, equal MMF is dropped across the centerpost and the outer legs, and the MMF between the windings is, according to a 1-D model, zero. With leakage excitation, the MMF's of the windings oppose each other, resulting in zero flux in the gaps, and so zero MMF at the outsides of the windings. In either case, one side of each winding has zero MMF, and $k = 1$. Thus, the one dimensional model predicts equal ac resistance for either leakage or magnetizing excitation. As shown in Fig. 6, the winding resistance in fact depends greatly on which connection is used, indicating once again that the 1-D model is not adequate for this geometry.

Acknowledgment

The author thanks J. Spreen, B. Hesterman, P. Wallmeier, and an anonymous reviewer for helpful comments; and Y. Lin for help with winding test transformers.

References

[1] S. Butterworth, "Effective resistance of inductance coils at radio frequency—Part I," *Wireless Eng.*, vol. 3, pp. 203–210, Apr. 1926.
[2] ——, "Effective resistance of inductance coils at radio frequency—Part II," *Wireless Eng.*, vol. 3, pp. 309–316, May 1926.
[3] ——, "Effective resistance of inductance coils at radio frequency—Part III," *Wireless Eng.*, vol. 3, pp. 417–424, July 1926.
[4] ——, "Effective resistance of inductance coils at radio frequency—Part IV," *Wireless Eng.*, vol. 3, pp. 483–492, Aug. 1926.
[5] G. W. O. Howe, "The high-frequency resistance of multiply-stranded insulated wire," in *Proc. R. Soc. London*, vol. XCII, Oct. 1917, pp. 468–492.
[6] J. A. Ferreira, "Improved analytical modeling of conductive losses in magnetic components," *IEEE Trans. Power Electron.*, vol. 9, pp. 127–131, Jan. 1994.
[7] P. L. Dowell, "Effects of eddy currents in transformer windings," *Proc. Inst. Elect. Eng.*, vol. 113, no. 8, pp. 1387–1394, Aug. 1966.
[8] J. Jongsma, "Minimum loss transformer windings for ultrasonic frequencies—Part 1: Background and theory," *Philips Electron. Applicat. Bull.*, vol. 35, no. 3, pp. 146–163, 1978.
[9] ——, "Minimum loss transformer windings for ultrasonic frequencies—Part 2: Transformer winding design," *Philips Electron. Applicat. Bull.*, vol. E.A.B. 35, no. 4, pp. 211–226, 1979.
[10] ——, "High frequency ferrite power transformer and choke design—Part 3: Transformer winding design," Philips, Eindhoven, The Netherlands, Tech. Rep. 207, 1986.
[11] P. S. Venkatraman, "Winding eddy current losses in switch mode power transformers due to rectangular wave currents," in *Proceedings of Powercon 11*. Dallas, TX: Power Concepts, Inc., 1984, pp. 1–11.
[12] N. R. Coonrod, "Transformer computer design aid for higher frequency switching power supplies," in *Proc. IEEE Power Electron. Spec. Conf. Rec.*, 1984, pp. 257–267.
[13] J. P. Vandelac and P. Ziogas, "A novel approach for minimizing high frequency transformer copper losses," in *IEEE Power Electron. Spec. Conf. Rec.*, 1987, pp. 355–367.
[14] L. H. Dixon, Jr., "Review of basic magnetics. Theory, conceptual models, and design equations," in *Unitrode Switching Regulated Power Supply Design Seminar Manual*. Merrimack, NH: Unitrode Corporation, 1988, pp. M4-1–M4-11.
[15] E. C. Snelling, *Soft Ferrites, Properties and Applications*, second ed. London, U.K.: Butterworths, 1988.
[16] A. M. Urling, V. A. Niemela, G. R. Skutt, and T. G. Wilson, "Characterizing high-frequency effects in transformer windings-A guide to several significant articles," in *Proc. APEC'89*, Mar. 1989, pp. 373–385.
[17] J. A. Ferreira, *Electromagnetic Modeling of Power Electronic Converters*. Norwell, MA: Kluwer, 1989.

[18] W. R. Smythe, *Static and Dynamic Electricity*. New York: McGraw-Hill, 1968, p. 411.
[19] P. N. Murgatroyd, "The torroidal cage coil," *Proc. Inst. Electron. Eng. B*, vol. 127, no. 4, pp. 207–214, 1980.
[20] S. Crepaz, "Eddy-current losses in rectifier transformers," *IEEE Trans. Power Apparat. Syst.*, vol. PAS-89, pp. 1651–1662, July 1970.
[21] C. R. Sullivan, "Optimal choice for number of strands in a litz-wire transformer winding," *IEEE Trans. Power Electron.*, vol. 14, pp. 283–291, Mar. 1999.
[22] J. M. Lopera, M. J. Prieto, F. Nuno, A. M. Pernia, and J. Sebastian, "A quick way to determine the optimum layer size and their disposition in magnetic structures," in *Proc. 28th Annu. IEEE Power Electron. Spec. Conf.*, 1997, pp. 1150–1156.
[23] W. G. Hurley, E. Gath, and J. G. Breslin, "Optimizing the ac resistance of multilayer transformer windings with arbitrary current waveforms," *IEEE Trans. Power Electron.*, vol. 15, pp. 369–376, Mar. 2000.
[24] R. Severns, "Additional losses in high frequency magnetics due to non ideal field distributions," in *Proc. APEC'92 7th Annu. IEEE Appl. Power Electron. Conf.*, 1992, pp. 333–338.
[25] P. Wallmeier, N. Frohleke, and H. Grotstollen, "Improved analytical modeling of conductive losses in gapped high-frequency inductors," in *Proc. 1998 IEEE Ind. Applicat. Soc. Annu. Meeting*, 1998, pp. 913–920.
[26] A. M. Tuckey, "Resonant link inverters for trapezoidal flux electrically commutated machines," Ph.D. dissertation, Northern Territory Univ., Beijing, China, 2000.
[27] J. Hu and C. R. Sullivan, "The quasidistributed gap technique for planar inductors: Design guidelines," in *Proc. 1997 IEEE Ind. Applicat. Soc. Annu. Meeting*, 1997, pp. 1147–1152.
[28] F. Robert, P. Mathys, and J.-P. Schauwers, "A closed-form formula for 2d ohmic losses calculation in smps transformer foils," in *Proc. APEC'99 14th Annu. Appl. Power Electron. Conf.*, 1999, pp. 199–205.
[29] J. Hu and C. R. Sullivan, "Optimization of shapes for round-wire high-frequency gapped-inductor windings," in *Proc. 1998 IEEE Ind. Applicat. Soc. Annu. Meeting*, 1998, pp. 900–906.
[30] B. Hesterman, "Time-domain k-factor computation methods," in *Proc. PCIM'94 29th Int. Power Conv. Conf.*, Sept. 1994, pp. 406–417.
[31] J. H. Spreen, "Electrical terminal representation of conductor loss in transformers," *IEEE Trans. Power Electron.*, vol. 5, pp. 424–429, July 1990.
[32] C. R. Sullivan, "Winding loss calculation with multiple windings, arbitrary waveforms, and 2-D field geometry," in *Proc. 1999 IEEE Ind. Applicat. Soc. Annu. Meeting*, 1999, pp. 2093–2099.
[33] Ansoft Corporation, Maxwell finite element analysis software, Pittsburgh, PA.

Charles R. Sullivan (M'93) was born in Princeton, NJ, in 1964. He received the B.S. degree in electrical engineering (with highest honors) from Princeton University, in 1987 and the Ph.D. degree in electrical engineering from the University of California, Berkeley, in 1996.

Between 1987 and 1990, he worked at Lutron Electronics, Coopersburg, PA, developing high frequency dimming ballasts for compact fluorescent lamps. He is presently Assistant Professor at the Thayer School of Engineering, Dartmouth College, Hanover, NH. He has published technical papers on topics including thin-film magnetics for high frequency power conversion; magnetic component design optimization; dc–dc converter topologies; energy and environmental issues; and modeling, analysis, and control of electric machines.

Dr. Sullivan received the National Science Foundation CAREER award in 1999 and a Power Electronics Society Prize Paper Award in 2000.